Supporting Information

B-site Octahedral Bridge and A-site Polyvalent Cu cations Related Electron Hopping in $LiCuNb_3O_9$-based Colossal Permittivity Materials

Dandan Gao, Jiyang Xie, Jian Wang* and Wanbiao Hu*

Key Laboratory of LCR Materials and Devices of Yunnan Province, National Center for International Research on Photoelectric and Energy Materials, School of Materials and Energy, Yunnan University, Kunming 650091, P. R. China

*Correspondence should be addressed:

Jian Wang (wang.jian@ynu.edu.cn)

Wanbiao Hu (huwanbiao@ynu.edu.cn)

Figure S1

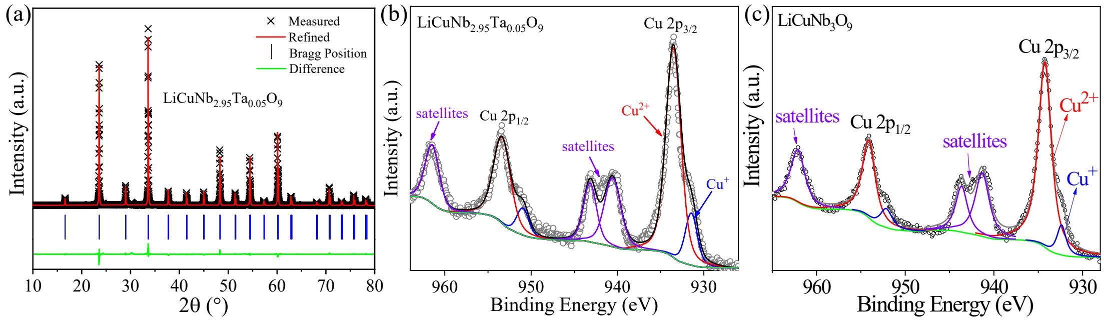

Figure S1. (a) Rietveld refinement results for $LiCuNb_{2.95}Ta_{0.05}O_9$ ceramic. (b, c) XPS spectrums of the Cu 2p peaks in $LiCuNb_{2.95}Ta_{0.05}O_9$ and $LiCuNb_3O_9$ ceramics.[1]

B-site isovalent-substituted compound $LiCuNb_{2.95}Ta_{0.05}O_9$ ceramic was synthesized by a solid-state reaction method. The power XRD (Figure S1a) shows there is a pure phase with a space group of *I*23, matching well with the PDF#81-2172. Refinement structure parameters *a*=*b*=*c*=7.5287 Å, are a little smaller than that of $LiCuNb_3O_9$. It's common in Nb/Ta-based oxides that the structure parameters decrease with increasing Ta content, which is because of Nb^{5+} ions are more greatly shifted than Ta^{5+} in the BO_6 octahedra, *i.e.* NbO_6 and TaO_6.[2, 3] As shown in Figures S1b-c, Cu^+ and Cu^{2+} are co-exist in both $LiCuNb_{2.95}Ta_{0.05}O_9$ and $LiCuNb_3O_9$ ceramics, and the ratio of Cu^+/Cu^{2+} in $LiCuNb_{2.95}Ta_{0.05}O_9$ is Cu^+:Cu^{2+}=19:81. There is no Cu^{3+} ion contained in the isovalent-substituted sample, which implying that only the acceptor doping induced the lack of charge is compensated by the fluctuation of Cu ions charge states, *i.e.* forming Cu^{3+} ions.

Figure S2

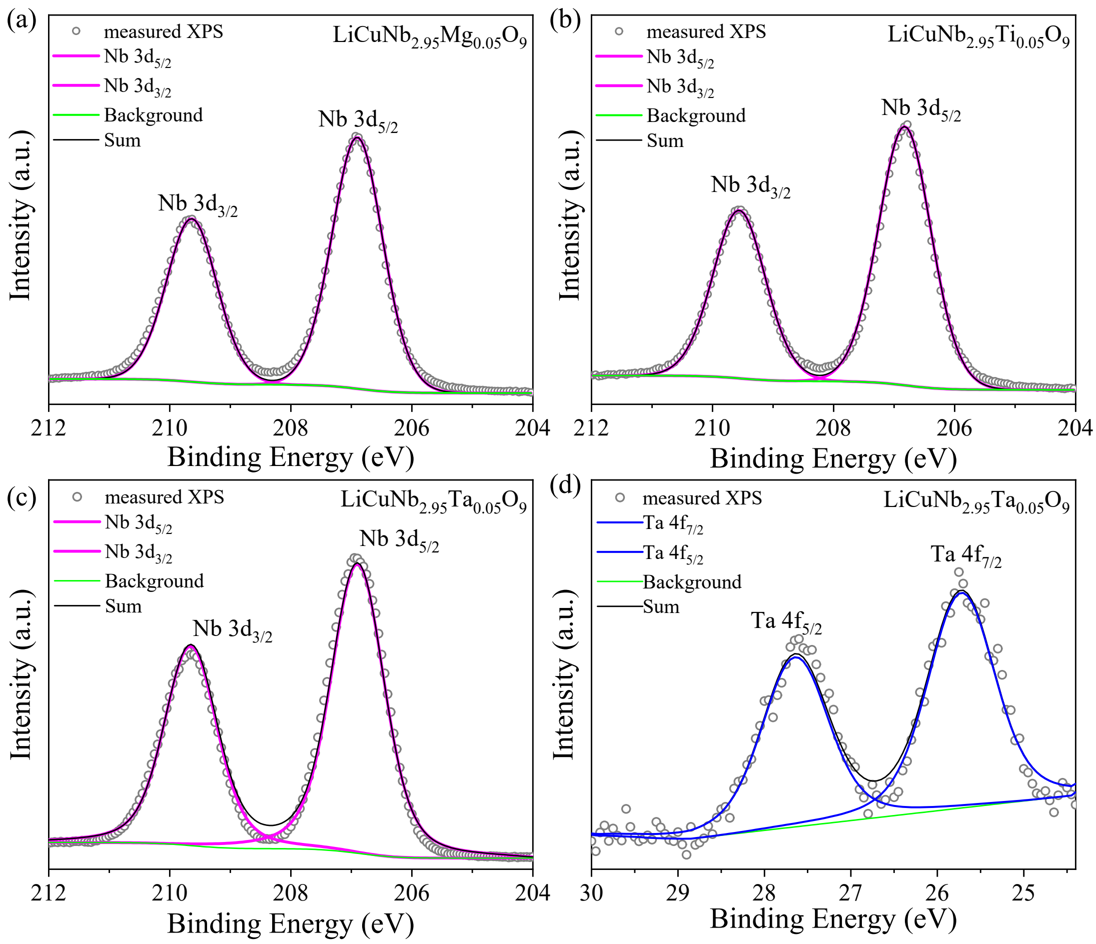

Figure S2. (a-c) XPS spectrums of Nb 3d peaks in $LiCuNb_{2.95}M_{0.05}O_9$ (*M*=Mg, Ti, Ta) ceramics. (d) XPS spectrums of Ta 4f peaks in $LiCuNb_{2.95}Ta_{0.05}O_9$ ceramic.

There is only Nb^{5+} valance state containing in all the B-site doping samples $LiCuNb_{2.95}M_{0.05}O_9$ (*M*=Mg, Ti, Ta). The Ta ions is pentavalent too in $LiCuNb_{2.95}Ta_{0.05}O_9$ ceramic.

Figure S3

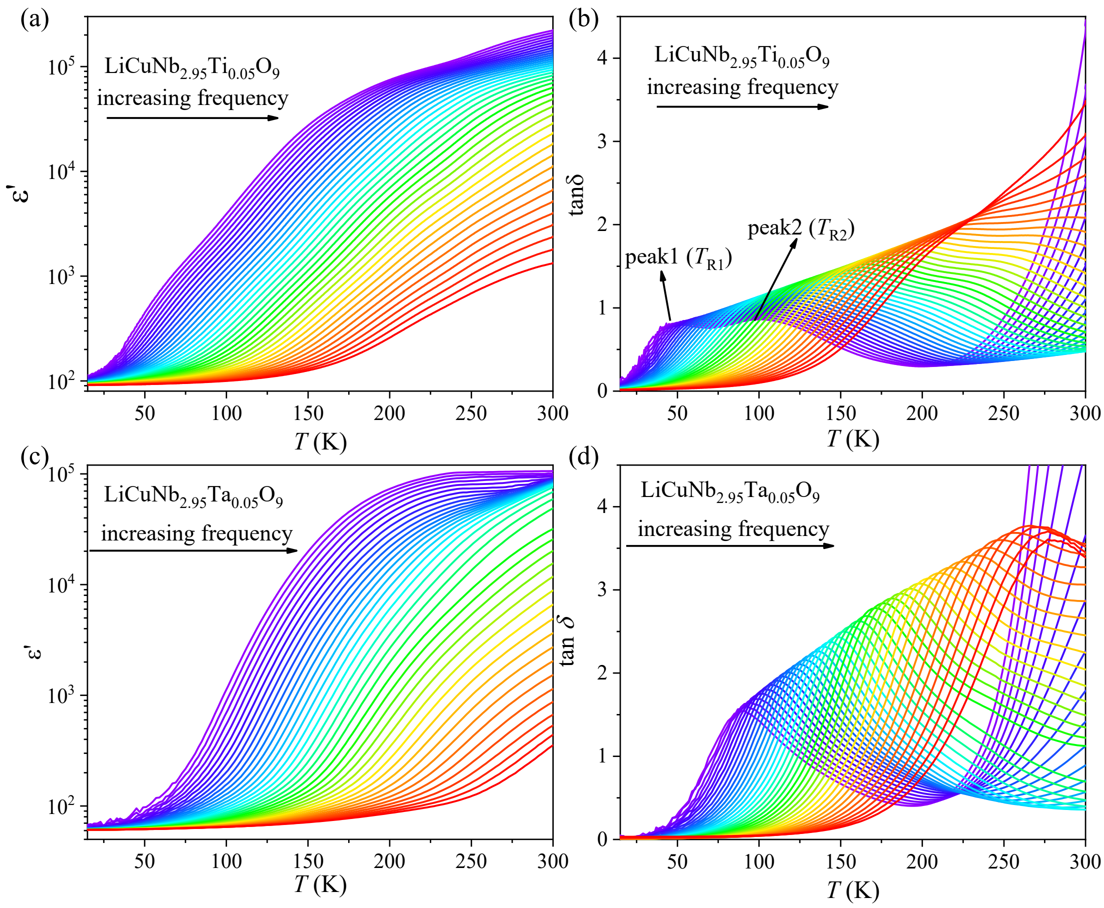

Figure S3. Temperature-dependent dielectric constants ε' (a, c) and dielectric loss tan*δ* (b, d) for $LiCuNb_{2.95}Ti_{0.05}O_9$ and $LiCuNb_{2.95}Ta_{0.05}O_9$ ceramics measured under different frequency (40 Hz - 1 MHz).

The dielectric spectra of $LiCuNb_{2.95}Ti_{0.05}O_9$ are similar to these of $LiCuNb_{2.95}Mg_{0.05}O_9$ ceramic. With increasing the temperatures, the dielectric constant increases gradually combining with two dielectric relaxations (T_{R1} and T_{R2}). Besides, the dielectric constant could reach the order of magnitude of 10^5 at room temperature. With increasing the frequencies, both of the dielectric peaks in tan*δ* spectra (Figure S3b) shift to higher temperatures. However, there is only one dielectric relaxation process for $LiCuNb_{2.95}Ta_{0.05}O_9$ ceramic with lower temperatures, which shifts higher temperatures with increasing test frequencies (Figure 3d). Similarly, in $LiCuNb_3O_9$ ceramic, one dielectric relaxation appears at low temperatures too, because of the variable range hopping coming from the A-site mixed valence states, *i.e.* Cu^+/Cu^{2+}.

Thus, it's reasonable to infer that the low temperature dielectric relaxation in $LiCuNb_{2.95}Ta_{0.05}O_9$ ceramic is also built by the Cu^{+}/Cu^{2+}. In conclusion, the acceptor doping in $LiCuNb_3O_9$ system, not only induces A-site polyvalent Cu ions, but also contributes to the two low temperature dielectric relaxations.

Figure S4

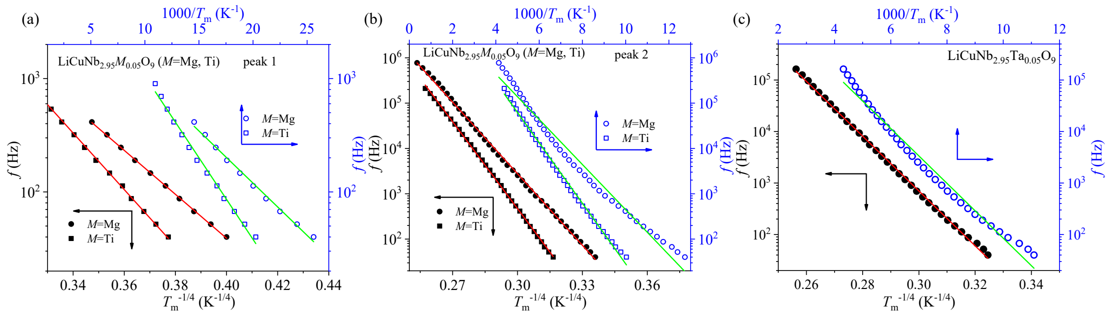

Figure S4. Temperature-dependent relaxation frequency f in $LiCuNb_{2.95}M_{0.05}O_9$ (M = Mg, Ti, Ta) ceramics with respect to $1/T_m$ (Arrhenius) and $1/T_m^{1/4}$ (Mott-VRH). (a) and (b) are the fitted results of peak 1 (T_{R1}) and peak 2 (T_{R2}), respectively. (c) the fitted results of $LiCuNb_{2.95}Ta_{0.05}O_9$ ceramic.

For T_{R1}, it follows variable range hopping model $f = f_0 \exp[-(T_0/T_m)^{1/4}]$ rather than the Arrhenius model $f = f_1 \exp(-\Delta E/k_B T_m)$ due to (1) the Arrhenius plot of f in Figure S4a doesn't lead to a straight line over significant temperature range, and the similar deviation has been found in series colossal permittivity system with low temperature polarons following VRH relation, and (2) the Arrhenius fitting gives unreasonable parameters (for $LiCuNb_{2.95}Mg_{0.05}O_9$ ΔE is 18.3 meV and f_1 is 8.32×10^3 Hz, but for $CaCu_3Ti_4O_{12}$ and $FeTiNbO_6$ are 67 meV ~ 1.19×10^7 Hz and 350 meV ~ 1.95×10^{10} Hz, respectively).[4, 5] Likewise, T_{R2} is considered to follow the VRH model as well and the experimental data deviates from Arrhenius law more significantly. The fitted parameters f_1, ΔE, f_0 and T_0 for $LiCuNb_{2.95}M_{0.05}O_9$ (M = Mg, Ti) samples are summarized in Table S1. For the reference sample $LiCuNb_{2.95}Ta_{0.05}O_9$ ceramic, temperature-dependent relaxation frequencies obey VRH model, and the fitted parameters are $f_0=6.4\times10^{18}$ Hz and $T_0=2.25\times10^8$ K, respectively, which are similar with those in pure $LiCuNb_3O_9$ ceramic. Thus, the B-site isovalent substitution in $LiCuNb_3O_9$ system not effects the dielectric relaxation significantly, but the acceptor doping could regulate the Cu ions species and make a difference in lower-temperature dielectric relaxation process.

Table S1

Table S1. The fitting parameters, *i.e.* f_1, ΔE, f_0 and T_0, of two dielectric-relaxation frequencies f versus relaxation temperature T_m by employing Arrhenius and Mott eqations.

$LiCuNb_{2.95}M_{0.05}O_9$	T_{R1}-low temperature				T_{R2}-high temperature			
	NNH		VRH		NNH		VRH	
	f_1 (Hz)	ΔE (meV)	f_0 (Hz)	T_0 (K)	f_1 (Hz)	ΔE (meV)	f_0 (Hz)	T_0 (K)
M=Mg	8.32×10^3	18.28	3.21×10^9	3.97×10^6	4.29×10^7	98.88	1.72×10^{19}	2.16×10^8
M=Ti	2.91×10^4	28.60	1.03×10^{11}	1.09×10^7	1.35×10^8	132.47	7.08×10^{21}	4.69×10^8

Table S2

Table S2. The fitting parameters of dc conductivity σ_{dc} versus temperature *T* by using VRH model.

$LiCuNb_{2.95}M_{0.05}O_9$	Temperature range (K)	VRH	
		σ_0 (S/cm)	T_0 (K)
M=Mg	20-100	1.17×10^{-3}	7.17×10^{5}
	110-240	4.40×10^{7}	1.30×10^{8}
M=Ti	20-100	7.48×10^{-4}	8.93×10^{5}
	110-240	1.17×10^{7}	1.35×10^{8}

References

1 D. Gao, J. Xie, X.-M. Jiang, H. Liu, G. Li, J. Wang, L. Zhang, F. Xiong and W. Hu, *ACS Appl. Electron. Mater.*, 2019, **1**, 64-74.

2 T. Nagai, Y. Mochizuki, H. Shirakuni, A. Nakano, F. Oba, I. Terasaki and H. Taniguchi, *Chem. Mater.*, 2020, **32**, 744-750.

3 M. Fukuda, I. Yamada, H. Hojo, C. Takahashi, Y. Yoshida, K. Tanaka, M. Azuma and K. Fujita, *J. Mater. Chem. C*, 2021, **9**, 13981-13990.

4 L. Ni and X. M. Chen, *Appl. Phys. Lett.*, 2007, **91**, 122905.

5 S. K. Deshpande, S. N. Achary, R. Mani, J. Gopalakrishnan and A. K. Tyagi, *Phys. Rev. B*, 2011, **84**, 064301.